

Abstract

We have performed a search for the leptonic B decay $B^+ \rightarrow \mu^+ \nu_\mu$ with data collected at the $\Upsilon(4S)$ resonance by the *BABAR* experiment at the PEP-II storage ring. With an integrated luminosity of approximately 81.4 fb^{-1} (88.4 million $B\bar{B}$ pairs), we find no convincing evidence for a signal and set a preliminary upper limit on the branching fraction of $\mathcal{B}(B^+ \rightarrow \mu^+ \nu_\mu) < 6.6 \times 10^{-6}$ at the 90% confidence level.

A search for $B^+ \rightarrow \mu^+ \nu_\mu$

The *BABAR* Collaboration

February 7, 2008

Abstract

We have performed a search for the leptonic decay $B^+ \rightarrow \mu^+ \nu_\mu$ with data collected at the $\Upsilon(4S)$ resonance by the *BABAR* experiment at the PEP-II storage ring. With an integrated luminosity of approximately 81.4 fb^{-1} (88.4 million $B\bar{B}$ pairs), we find no convincing evidence for a signal and set a preliminary upper limit on the branching fraction of $\mathcal{B}(B^+ \rightarrow \mu^+ \nu_\mu) < 6.6 \times 10^{-6}$ at the 90% confidence level.

Presented at the International Europhysics Conference On High-Energy Physics (HEP 2003),
7/17—7/23/2003, Aachen, Germany

Stanford Linear Accelerator Center, Stanford University, Stanford, CA 94309

Work supported in part by Department of Energy contract DE-AC03-76SF00515.

The BABAR Collaboration,

B. Aubert, R. Barate, D. Boutigny, J.-M. Gaillard, A. Hicheur, Y. Karyotakis, J. P. Lees, P. Robbe,
V. Tisserand, A. Zghiche

Laboratoire de Physique des Particules, F-74941 Annecy-le-Vieux, France

A. Palano, A. Pompili

Università di Bari, Dipartimento di Fisica and INFN, I-70126 Bari, Italy

J. C. Chen, N. D. Qi, G. Rong, P. Wang, Y. S. Zhu

Institute of High Energy Physics, Beijing 100039, China

G. Eigen, I. Ofte, B. Stugu

University of Bergen, Inst. of Physics, N-5007 Bergen, Norway

G. S. Abrams, A. W. Borgland, A. B. Breon, D. N. Brown, J. Button-Shafer, R. N. Cahn, E. Charles,
C. T. Day, M. S. Gill, A. V. Gritsan, Y. Groysman, R. G. Jacobsen, R. W. Kadel, J. Kadyk, L. T. Kerth,
Yu. G. Kolomensky, J. F. Kral, G. Kukartsev, C. LeClerc, M. E. Levi, G. Lynch, L. M. Mir, P. J. Oddone,
T. J. Orimoto, M. Pripstein, N. A. Roe, A. Romosan, M. T. Ronan, V. G. Shelkov, A. V. Telnov,
W. A. Wenzel

Lawrence Berkeley National Laboratory and University of California, Berkeley, CA 94720, USA

K. Ford, T. J. Harrison, C. M. Hawkes, D. J. Knowles, S. E. Morgan, R. C. Penny, A. T. Watson,
N. K. Watson

University of Birmingham, Birmingham, B15 2TT, United Kingdom

T. Deppermann, K. Goetzen, H. Koch, B. Lewandowski, M. Pelizaeus, K. Peters, H. Schmuecker,
M. Steinke

Ruhr Universität Bochum, Institut für Experimentalphysik 1, D-44780 Bochum, Germany

N. R. Barlow, J. T. Boyd, N. Chevalier, W. N. Cottingham, M. P. Kelly, T. E. Latham, C. Mackay,
F. F. Wilson

University of Bristol, Bristol BS8 1TL, United Kingdom

K. Abe, T. Cuhadar-Donszelmann, C. Hearty, T. S. Mattison, J. A. McKenna, D. Thiessen

University of British Columbia, Vancouver, BC, Canada V6T 1Z1

P. Kyberd, A. K. McKemey

Brunel University, Uxbridge, Middlesex UB8 3PH, United Kingdom

V. E. Blinov, A. D. Bukin, V. B. Golubev, V. N. Ivanchenko, E. A. Kravchenko, A. P. Onuchin,
S. I. Serednyakov, Yu. I. Skovpen, E. P. Solodov, A. N. Yushkov

Budker Institute of Nuclear Physics, Novosibirsk 630090, Russia

D. Best, M. Bruinsma, M. Chao, D. Kirkby, A. J. Lankford, M. Mandelkern, R. K. Mommsen, W. Roethel,
D. P. Stoker

University of California at Irvine, Irvine, CA 92697, USA

C. Buchanan, B. L. Hartfiel

University of California at Los Angeles, Los Angeles, CA 90024, USA

B. C. Shen

University of California at Riverside, Riverside, CA 92521, USA

D. del Re, H. K. Hadavand, E. J. Hill, D. B. MacFarlane, H. P. Paar, Sh. Rahatlou, U. Schwanke,
V. Sharma

University of California at San Diego, La Jolla, CA 92093, USA

J. W. Berryhill, C. Campagnari, B. Dahmes, N. Kuznetsova, S. L. Levy, O. Long, A. Lu, M. A. Mazur,
J. D. Richman, W. Verkerke

University of California at Santa Barbara, Santa Barbara, CA 93106, USA

T. W. Beck, J. Beringer, A. M. Eisner, C. A. Heusch, W. S. Lockman, T. Schalk, R. E. Schmitz,
B. A. Schumm, A. Seiden, M. Turri, W. Walkowiak, D. C. Williams, M. G. Wilson

University of California at Santa Cruz, Institute for Particle Physics, Santa Cruz, CA 95064, USA

J. Albert, E. Chen, G. P. Dubois-Felsmann, A. Dvoretzskii, D. G. Hitlin, I. Narsky, F. C. Porter, A. Ryd,
A. Samuel, S. Yang

California Institute of Technology, Pasadena, CA 91125, USA

S. Jayatilke, G. Mancinelli, B. T. Meadows, M. D. Sokoloff

University of Cincinnati, Cincinnati, OH 45221, USA

T. Abe, F. Blanc, P. Bloom, S. Chen, P. J. Clark, W. T. Ford, U. Nauenberg, A. Olivas, P. Rankin, J. Roy,
J. G. Smith, W. C. van Hoek, L. Zhang

University of Colorado, Boulder, CO 80309, USA

J. L. Harton, T. Hu, A. Soffer, W. H. Toki, R. J. Wilson, J. Zhang

Colorado State University, Fort Collins, CO 80523, USA

D. Altenburg, T. Brandt, J. Brose, T. Colberg, M. Dickopp, R. S. Dubitzky, A. Hauke, H. M. Lackner,
E. Maly, R. Müller-Pfefferkorn, R. Nogowski, S. Otto, J. Schubert, K. R. Schubert, R. Schwierz, B. Spaan,
L. Wilden

Technische Universität Dresden, Institut für Kern- und Teilchenphysik, D-01062 Dresden, Germany

D. Bernard, G. R. Bonneaud, F. Brochard, J. Cohen-Tanugi, P. Grenier, Ch. Thiebaux, G. Vasileiadis,
M. Verderi

Ecole Polytechnique, LLR, F-91128 Palaiseau, France

A. Khan, D. Lavin, F. Muheim, S. Playfer, J. E. Swain, J. Tinslay

University of Edinburgh, Edinburgh EH9 3JZ, United Kingdom

M. Andreotti, V. Azzolini, D. Bettoni, C. Bozzi, R. Calabrese, G. Cibinetto, E. Luppi, M. Negrini,
L. Piemontese, A. Sarti

Università di Ferrara, Dipartimento di Fisica and INFN, I-44100 Ferrara, Italy

E. Treadwell

Florida A&M University, Tallahassee, FL 32307, USA

F. Anulli,¹ R. Baldini-Ferroli, M. Biasini,¹ A. Calcaterra, R. de Sangro, D. Falciari, G. Finocchiaro,
P. Patteri, I. M. Peruzzi,¹ M. Piccolo, M. Pioppi,¹ A. Zallo

Laboratori Nazionali di Frascati dell'INFN, I-00044 Frascati, Italy

A. Buzzo, R. Capra, R. Contri, G. Crosetti, M. Lo Vetere, M. Macri, M. R. Monge, S. Passaggio,
C. Patrignani, E. Robutti, A. Santroni, S. Tosi

Università di Genova, Dipartimento di Fisica and INFN, I-16146 Genova, Italy

S. Bailey, M. Morii, E. Won

Harvard University, Cambridge, MA 02138, USA

W. Bhimji, D. A. Bowerman, P. D. Dauncey, U. Egede, I. Eschrich, J. R. Gaillard, G. W. Morton,
J. A. Nash, P. Sanders, G. P. Taylor

Imperial College London, London, SW7 2BW, United Kingdom

G. J. Grenier, S.-J. Lee, U. Mallik

University of Iowa, Iowa City, IA 52242, USA

J. Cochran, H. B. Crawley, J. Lamsa, W. T. Meyer, S. Prell, E. I. Rosenberg, J. Yi

Iowa State University, Ames, IA 50011-3160, USA

M. Davier, G. Grosdidier, A. Höcker, S. Laplace, F. Le Diberder, V. Lepeltier, A. M. Lutz, T. C. Petersen,
S. Plaszczynski, M. H. Schune, L. Tantot, G. Wormser

Laboratoire de l'Accélérateur Linéaire, F-91898 Orsay, France

V. Brigljević, C. H. Cheng, D. J. Lange, D. M. Wright

Lawrence Livermore National Laboratory, Livermore, CA 94550, USA

A. J. Bevan, J. P. Coleman, J. R. Fry, E. Gabathuler, R. Gamet, M. Kay, R. J. Parry, D. J. Payne,
R. J. Sloane, C. Touramanis

University of Liverpool, Liverpool L69 3BX, United Kingdom

J. J. Back, P. F. Harrison, H. W. Shorthouse, P. Strother, P. B. Vidal

Queen Mary, University of London, E1 4NS, United Kingdom

C. L. Brown, G. Cowan, R. L. Flack, H. U. Flaecher, S. George, M. G. Green, A. Kurup, C. E. Marker,
T. R. McMahon, S. Ricciardi, F. Salvatore, G. Vaitsas, M. A. Winter

University of London, Royal Holloway and Bedford New College, Egham, Surrey TW20 0EX, United Kingdom

D. Brown, C. L. Davis

University of Louisville, Louisville, KY 40292, USA

J. Allison, R. J. Barlow, A. C. Forti, P. A. Hart, F. Jackson, G. D. Lafferty, A. J. Lyon, J. H. Weatherall,
J. C. Williams

University of Manchester, Manchester M13 9PL, United Kingdom

A. Farbin, A. Jawahery, D. Kovalskyi, C. K. Lae, V. Lillard, D. A. Roberts

University of Maryland, College Park, MD 20742, USA

¹Also with Università di Perugia, Perugia, Italy

G. Blaylock, C. Dallapiccola, K. T. Flood, S. S. Hertzbach, R. Kofler, V. B. Koptchev, T. B. Moore,
S. Saremi, H. Staengle, S. Willocq

University of Massachusetts, Amherst, MA 01003, USA

R. Cowan, G. Sciolla, F. Taylor, R. K. Yamamoto

Massachusetts Institute of Technology, Laboratory for Nuclear Science, Cambridge, MA 02139, USA

D. J. J. Mangeol, M. Milek, P. M. Patel

McGill University, Montréal, QC, Canada H3A 2T8

A. Lazzaro, F. Palombo

Università di Milano, Dipartimento di Fisica and INFN, I-20133 Milano, Italy

J. M. Bauer, L. Cremaldi, V. Eschenburg, R. Godang, R. Kroeger, J. Reidy, D. A. Sanders, D. J. Summers,
H. W. Zhao

University of Mississippi, University, MS 38677, USA

S. Brunet, D. Cote-Ahern, C. Hast, P. Taras

Université de Montréal, Laboratoire René J. A. Lévesque, Montréal, QC, Canada H3C 3J7

H. Nicholson

Mount Holyoke College, South Hadley, MA 01075, USA

C. Cartaro, N. Cavallo,² G. De Nardo, F. Fabozzi,² C. Gatto, L. Lista, P. Paolucci, D. Piccolo, C. Sciacca
Università di Napoli Federico II, Dipartimento di Scienze Fisiche and INFN, I-80126, Napoli, Italy

M. A. Baak, G. Raven

NIKHEF, National Institute for Nuclear Physics and High Energy Physics, NL-1009 DB Amsterdam, The Netherlands

J. M. LoSecco

University of Notre Dame, Notre Dame, IN 46556, USA

T. A. Gabriel

Oak Ridge National Laboratory, Oak Ridge, TN 37831, USA

B. Brau, K. K. Gan, K. Honscheid, D. Hufnagel, H. Kagan, R. Kass, T. Pulliam, Q. K. Wong

Ohio State University, Columbus, OH 43210, USA

J. Brau, R. Frey, C. T. Potter, N. B. Sinev, D. Strom, E. Torrence

University of Oregon, Eugene, OR 97403, USA

F. Colecchia, A. Dorigo, F. Galeazzi, M. Margoni, M. Morandin, M. Posocco, M. Rotondo, F. Simonetto,
R. Stroili, G. Tiozzo, C. Voci

Università di Padova, Dipartimento di Fisica and INFN, I-35131 Padova, Italy

M. Benayoun, H. Briand, J. Chauveau, P. David, Ch. de la Vaissière, L. Del Buono, O. Hamon,
M. J. J. John, Ph. Leruste, J. Ocariz, M. Pivk, L. Roos, J. Stark, S. T'Jampens, G. Therin

Universités Paris VI et VII, Lab de Physique Nucléaire H. E., F-75252 Paris, France

²Also with Università della Basilicata, Potenza, Italy

P. F. Manfredi, V. Re

Università di Pavia, Dipartimento di Elettronica and INFN, I-27100 Pavia, Italy

P. K. Behera, L. Gladney, Q. H. Guo, J. Panetta

University of Pennsylvania, Philadelphia, PA 19104, USA

C. Angelini, G. Batignani, S. Bettarini, M. Bondioli, F. Bucci, G. Calderini, M. Carpinelli, F. Forti,
M. A. Giorgi, A. Lusiani, G. Marchiori, F. Martinez-Vidal,³ M. Morganti, N. Neri, E. Paoloni, M. Rama,
G. Rizzo, F. Sandrelli, J. Walsh

Università di Pisa, Dipartimento di Fisica, Scuola Normale Superiore and INFN, I-56127 Pisa, Italy

M. Haire, D. Judd, K. Paick, D. E. Wagoner

Prairie View A&M University, Prairie View, TX 77446, USA

N. Danielson, P. Elmer, C. Lu, V. Miftakov, J. Olsen, A. J. S. Smith, H. A. Tanaka, E. W. Varnes

Princeton University, Princeton, NJ 08544, USA

F. Bellini, G. Cavoto,⁴ R. Faccini,⁵ F. Ferrarotto, F. Ferroni, M. Gaspero, M. A. Mazzoni, S. Morganti,
M. Pierini, G. Piredda, F. Safai Tehrani, C. Voena

Università di Roma La Sapienza, Dipartimento di Fisica and INFN, I-00185 Roma, Italy

S. Christ, G. Wagner, R. Waldi

Universität Rostock, D-18051 Rostock, Germany

T. Adye, N. De Groot, B. Franek, N. I. Geddes, G. P. Gopal, E. O. Olaiya, S. M. Xella

Rutherford Appleton Laboratory, Chilton, Didcot, Oxon, OX11 0QX, United Kingdom

R. Aleksan, S. Emery, A. Gaidot, S. F. Ganzhur, P.-F. Giraud, G. Hamel de Monchenault, W. Kozanecki,
M. Langer, M. Legendre, G. W. London, B. Mayer, G. Schott, G. Vasseur, Ch. Yeche, M. Zito

DSM/Daphnia, CEA/Saclay, F-91191 Gif-sur-Yvette, France

M. V. Purohit, A. W. Weidemann, F. X. Yumiceva

University of South Carolina, Columbia, SC 29208, USA

D. Aston, R. Bartoldus, N. Berger, A. M. Boyarski, O. L. Buchmueller, M. R. Convery, D. P. Coupal,
D. Dong, J. Dorfan, D. Dujmic, W. Dunwoodie, R. C. Field, T. Glanzman, S. J. Gowdy, E. Grauges-Pous,
T. Hadig, V. Halyo, T. Hryn'ova, W. R. Innes, C. P. Jessop, M. H. Kelsey, P. Kim, M. L. Kocian,
U. Langenegger, D. W. G. S. Leith, S. Luitz, V. Luth, H. L. Lynch, H. Marsiske, R. Messner, D. R. Muller,
C. P. O'Grady, V. E. Ozcan, A. Perazzo, M. Perl, S. Petrak, B. N. Ratcliff, S. H. Robertson, A. Roodman,
A. A. Salnikov, R. H. Schindler, J. Schwiening, G. Simi, A. Snyder, A. Soha, J. Stelzer, D. Su,
M. K. Sullivan, J. Va'vra, S. R. Wagner, M. Weaver, A. J. R. Weinstein, W. J. Wisniewski, D. H. Wright,
C. C. Young

Stanford Linear Accelerator Center, Stanford, CA 94309, USA

P. R. Burchat, A. J. Edwards, T. I. Meyer, B. A. Petersen, C. Roat

Stanford University, Stanford, CA 94305-4060, USA

³Also with IFIC, Instituto de Física Corpuscular, CSIC-Universidad de Valencia, Valencia, Spain

⁴Also with Princeton University

⁵Also with University of California at San Diego

S. Ahmed, M. S. Alam, J. A. Ernst, M. Saleem, F. R. Wappler
State Univ. of New York, Albany, NY 12222, USA

W. Bugg, M. Krishnamurthy, S. M. Spanier
University of Tennessee, Knoxville, TN 37996, USA

R. Eckmann, H. Kim, J. L. Ritchie, R. F. Schwitters
University of Texas at Austin, Austin, TX 78712, USA

J. M. Izen, I. Kitayama, X. C. Lou, S. Ye
University of Texas at Dallas, Richardson, TX 75083, USA

F. Bianchi, M. Bona, F. Gallo, D. Gamba
Università di Torino, Dipartimento di Fisica Sperimentale and INFN, I-10125 Torino, Italy

C. Borean, L. Bosisio, G. Della Ricca, S. Dittongo, S. Grancagnolo, L. Lanceri, P. Poropat,⁶ L. Vitale,
G. Vuagnin
Università di Trieste, Dipartimento di Fisica and INFN, I-34127 Trieste, Italy

R. S. Panvini
Vanderbilt University, Nashville, TN 37235, USA

Sw. Banerjee, C. M. Brown, D. Fortin, P. D. Jackson, R. Kowalewski, J. M. Roney
University of Victoria, Victoria, BC, Canada V8W 3P6

H. R. Band, S. Dasu, M. Datta, A. M. Eichenbaum, J. R. Johnson, P. E. Kutter, H. Li, R. Liu,
F. Di Lodovico, A. Mihalyi, A. K. Mohapatra, Y. Pan, R. Prepost, S. J. Sekula, J. H. von
Wimmersperg-Toeller, J. Wu, S. L. Wu, Z. Yu
University of Wisconsin, Madison, WI 53706, USA

H. Neal
Yale University, New Haven, CT 06511, USA

⁶Deceased

1 INTRODUCTION

The purely leptonic decays $B^+ \rightarrow \ell^+ \nu_\ell$ ($\ell = e, \mu$, or τ) proceed through the annihilation (Fig. 1) of the quark-antiquark pair in the meson to form a virtual W boson. In the Standard Model (SM), the branching fraction can be calculated as ¹,

$$\mathcal{B}(B^+ \rightarrow \ell^+ \nu_\ell) = \frac{G_F^2 m_B m_\ell^2}{8\pi} \left(1 - \frac{m_\ell^2}{m_B^2}\right)^2 f_B^2 |V_{ub}|^2 \tau_B, \quad (1)$$

where G_F is the Fermi coupling constant, m_ℓ and m_B are the lepton and B meson masses, and τ_B is the B^+ lifetime. The decay rate is sensitive to both the Cabibbo-Kobayashi-Maskawa matrix element V_{ub} and the B decay constant f_B which describes the overlap of the quark wave functions within the meson. Once $|V_{ub}|$ has been more precisely measured in B semi-leptonic decays, f_B could be extracted from a measurement of the $B^+ \rightarrow \ell^+ \nu_\ell$ branching fraction. Currently, the uncertainty on f_B is one of the main factors limiting the determination of $|V_{td}|$ from precision $B^0 \bar{B}^0$ mixing measurements.

The Standard Model estimate of the branching fraction for $B^+ \rightarrow \tau^+ \nu_\tau$ is about 9×10^{-5} assuming $\tau_B = 1.674$ ps, $|V_{ub}| = 0.0036$ and $f_B = 198$ MeV [1]. Due to helicity suppression, the expected branching fraction for $B^+ \rightarrow \mu^+ \nu_\mu$ is reduced to roughly 4×10^{-7} . However, physics beyond the Standard Model could substantially increase these predictions. Charged Higgs boson effects may greatly enhance the branching fraction in certain two Higgs doublet models [2]. Similarly, this decay may be enhanced through mediation by leptoquarks in the Pati-Salam model of quark-lepton unification [3].

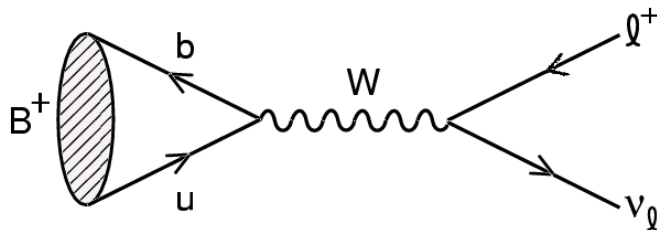


Figure 1: The SM $B^+ \rightarrow \ell^+ \nu_\ell$ annihilation diagram.

Purely leptonic B decays have not yet been observed experimentally. The CLEO [4] and Belle Collaborations [5] have set 90% confidence level upper limits on the $B^+ \rightarrow \mu^+ \nu_\mu$ branching fraction. The most stringent limit is currently from Belle,

$$\mathcal{B}(B^+ \rightarrow \mu^+ \nu_\mu) < 6.8 \times 10^{-6}$$

using 60 fb^{-1} of data collected at the $\Upsilon(4S)$ resonance.

2 THE BABAR DETECTOR AND DATASET

The data used in this analysis were collected with the *BABAR* detector at the PEP-II storage ring. The sample consists of an integrated luminosity of 81.4 fb^{-1} accumulated at the $\Upsilon(4S)$

¹Charge-conjugation is implied throughout this paper.

resonance and 9.6 fb^{-1} accumulated at a center-of-mass (CM) energy about 40 MeV below the $\Upsilon(4S)$ resonance. The on-resonance sample corresponds to about 88.4 million $B\bar{B}$ pairs. The collider is operated with asymmetric beam energies, producing a boost of the $\Upsilon(4S)$ along the collision axis of $\beta\gamma = 0.55$ in the laboratory frame.

The *BABAR* detector is optimized for the asymmetric-energy beams at PEP-II and is described in detail elsewhere [6]. Charged particle momentum and direction are measured with a 5-layer double-sided silicon vertex tracker (SVT) and a 40-layer drift chamber (DCH) which are contained in the 1.5 T magnetic field of a superconducting solenoid. Located just outside the DCH, a detector of internally reflected Cherenkov radiation (DIRC) provides separation of K^+ and π^+ . The energies of neutral particles are measured by the electromagnetic calorimeter (EMC) which is constructed of 6580 CsI(Tl) crystals. The flux return of the solenoid is instrumented with resistive plate chambers (IFR) for the identification of muons and K_L^0 . Averaged over the momentum and polar angle distributions of muons from $B^+ \rightarrow \mu^+\nu_\mu$, the muon identification efficiency is about 61% with a pion misidentification probability of about 2%.

A Geant4 based Monte Carlo (MC) simulation was used to optimize the signal selection criteria. A sample of 52,000 simulated B^+B^- events where $B^+ \rightarrow \mu^+\nu_\mu$ and the B^- decayed generically has been studied. Background sources considered include $e^+e^- \rightarrow B\bar{B}$, $e^+e^- \rightarrow q\bar{q}$ ($q = u, d, s$, and c), and $e^+e^- \rightarrow \tau^+\tau^-$ in quantities comparable to the data luminosity.

3 ANALYSIS METHOD

$B^+ \rightarrow \mu^+\nu_\mu$ is a two-body decay so the muon must be mono-energetic in the B rest frame. The momentum of the muon is given by

$$p^* = \frac{m_B^2 - m_\mu^2}{2m_B} \approx \frac{m_B}{2}. \quad (2)$$

At *BABAR*, the CM frame is a good approximation to the B rest frame so we initially select well-identified muon candidates with momentum p_{CM} between 2.25 and 2.95 GeV/ c in the CM frame. Since the neutrino produced in the signal decay is not detected, any other charged tracks or neutral energy in a signal event must have been produced by the decay of the companion B . Therefore, the companion B can be reconstructed from the remaining visible energy in the event. Signal decays can then be selected using the kinematic variables ΔE and energy-substituted mass, m_{ES} , defined by

$$\Delta E = E_B - E_{\text{beam}}, \quad (3)$$

and

$$m_{ES} = \sqrt{E_{\text{beam}}^2 - |\vec{p}_B|^2}, \quad (4)$$

where \vec{p}_B and E_B are the momentum and energy of the reconstructed companion B candidate in the CM frame and E_{beam} is the beam energy in the CM frame. The reconstruction of the companion B includes all charged tracks whose distance of closest approach to the beam-spot is less than 1.5 cm in the xy plane and within 10 cm along the beam axis. We also include all neutral calorimeter clusters with cluster energy greater than 30 MeV. Particle identification is applied to the charged tracks to identify electrons, muons, kaons and protons in order to apply the appropriate mass hypothesis to each track and thus improve the ΔE and m_{ES} resolution. In addition, events with additional identified leptons are discarded to discriminate against events containing additional neutrinos. The MC indicates that this requirement removes about 24% of the

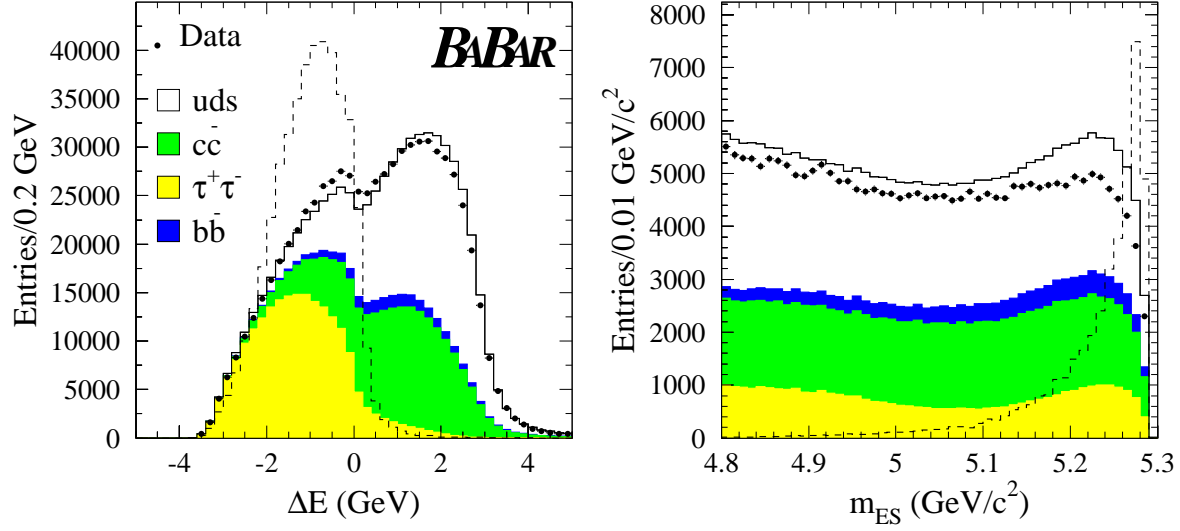


Figure 2: The distributions of ΔE and m_{ES} for on-peak data and MC after muon candidate selection. The signal distributions are overlaid (dashed histograms) with an arbitrary normalization.

signal decays. Figure 2 shows the distributions of ΔE and m_{ES} for the on-peak data, background MC and signal MC after muon candidate selection. For a signal decay, we expect the energy of the companion B to be consistent with the beam energy in the CM frame so that ΔE peaks near 0. Due to energy losses from detector acceptance, neutral hadrons and additional neutrinos, this distribution is shifted toward negative ΔE . We expect that m_{ES} should peak near the B mass for signal decays.

Once the companion B is reconstructed, we make a refined estimate of the muon momentum in the B “rest” frame. We use the momentum direction of the companion B and assume a total momentum of 320 MeV/c in the CM frame (from the decay of the $\Upsilon(4S) \rightarrow B\bar{B}$) to boost the muon candidate into the reconstructed B rest frame. Figure 3 shows the muon candidate momentum distribution in the B rest frame, p^* , for all muon candidates in the signal MC. The dashed curve is the momentum distribution of the same events in the CM frame.

Backgrounds may arise from any process producing charged tracks in the momentum range of the signal, particularly if the charged tracks are true muons. The two most significant backgrounds are the B semi-leptonic decays involving $b \rightarrow u\mu\nu$ transitions where the endpoint of the muon spectrum approaches that of the signal, and non-resonant $q\bar{q}$ (continuum) events where a charged pion is mistakenly identified as a muon. In the continuum events, there must also be significant missing energy due to detector acceptance, neutral hadrons, or additional neutrinos that mimic the signature of the expected neutrino. We are able to reduce these backgrounds by tightening the selection on the muon candidate momentum to $2.58 < p^* < 2.78$ GeV/c. The cut is asymmetric about the signal peak due to the decreasing momentum distribution of the backgrounds.

Continuum backgrounds are further suppressed using event shape variables. The light-quark events tend to produce a jet-like event topology as opposed to $B\bar{B}$ events which tend to be more

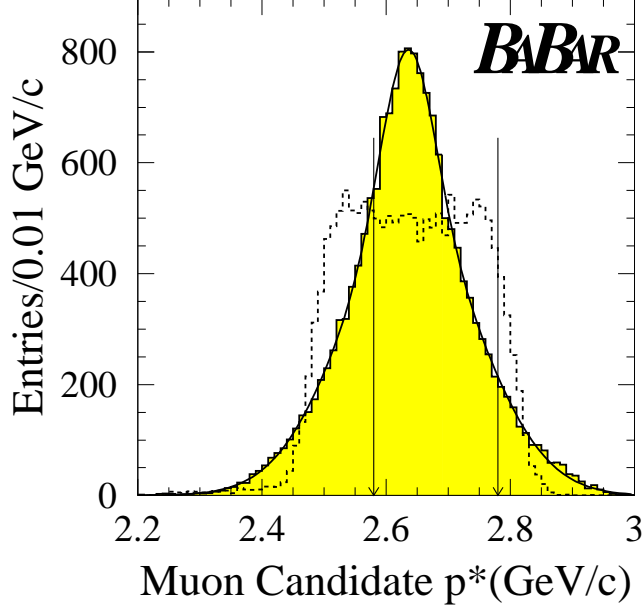


Figure 3: The muon candidate momentum distribution in the reconstructed B rest frame for all muon candidates in the signal MC. The dashed curve is the momentum distribution of the same events in the CM frame. The arrows indicate the selected signal region.

spherical. We define a variable, θ^T , which is the angle between the muon candidate momentum and the thrust axis of the rest of the event in the CM frame. For continuum background, $|\cos \theta^T|$ peaks sharply near one while the distribution is nearly flat for signal decays. By requiring $|\cos \theta^T| < 0.55$, we are able to remove about 98% of the continuum background while retaining about 53% of the signal decays. We also use the direction of the missing momentum in the laboratory frame to discriminate against continuum backgrounds. The missing 4-momentum is calculated as

$$P^\nu = P^{\Upsilon(4S)} - P^B - P^\mu, \quad (5)$$

where $P^{\Upsilon(4S)}$ is determined from the beam energies, and P^B and P^μ represent the reconstructed companion B and signal muon candidate respectively. In continuum decays, the missing momentum is often due to undetected particles that were outside the detector acceptance so that the polar angle of the missing momentum, θ^ν , lies near the beam axis. Therefore, we require $|\cos \theta^\nu| < 0.88$ so that the missing momentum is directed into the detector's fiducial volume. In addition, we require that the event contains at least four charged tracks and that the normalized second Fox-Wolfman moment [7] is less than 0.98. Figure 4 shows the on-peak data and MC distributions of $|\cos \theta^T|$ and $|\cos \theta^\nu|$. The events in these plots have passed the requirement $2.58 < p^* < 2.78$ GeV/c. For comparison, the signal MC is overlaid with an arbitrary normalization. The remaining $B\bar{B}$ background is not visible due to the earlier requirement on p^* .

We select $B^+ \rightarrow \mu^+ \nu_\mu$ signal events with simultaneous requirements on ΔE and m_{ES} , thus forming a “signal box.” The dimensions of the signal box, as well as the above requirements on p^* , $|\cos \theta^T|$ and $|\cos \theta^\nu|$, were determined using an optimization procedure that searches the cut-parameter space to find the combination of cuts that maximizes the quantity $S/\sqrt{S+B}$ where S

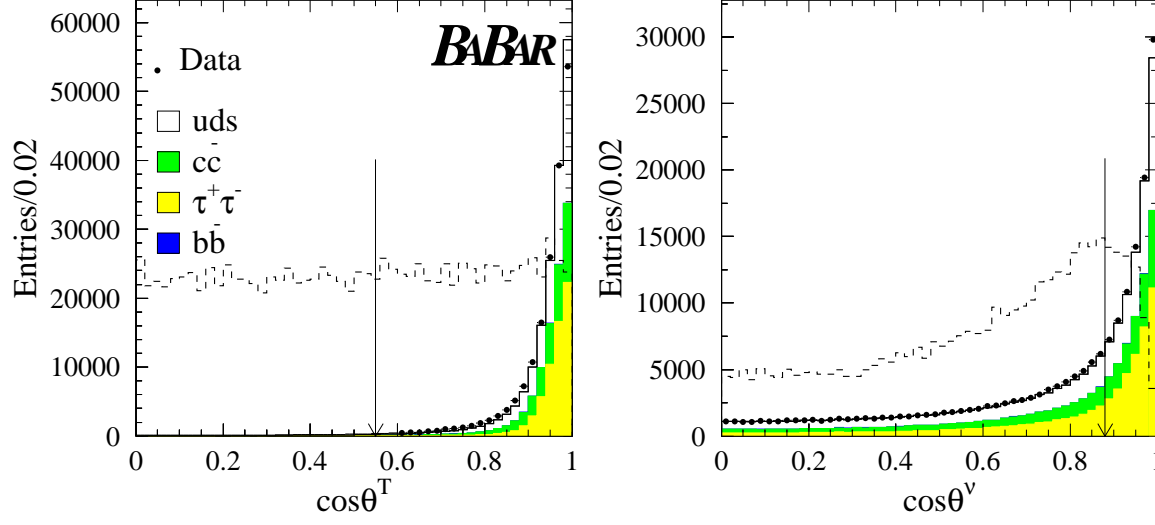


Figure 4: The distributions of $|\cos\theta^T|$ and $|\cos\theta^\nu|$ for on-peak data and MC. The events in these plots have passed the requirement $2.58 < p^* < 2.78$ GeV/c. The signal distributions are overlaid (dashed histograms) with an arbitrary normalization.

and B are the expected signal and background yields in the MC respectively. The signal branching fraction was set to 3×10^{-7} during the optimization procedure. The resulting box is defined by $-0.75 < \Delta E < 0.5$ GeV and $m_{\text{ES}} > 5.27$ GeV/ c^2 . The MC suggests that about 25% of signal decays passing all previous cuts fall within the signal box. After applying all selection criteria, the $B^+ \rightarrow \mu^+ \nu_\mu$ efficiency is determined from the MC to be 2.24 ± 0.07 % where the uncertainty is due to MC statistics. Figure 6(a) shows the distribution of ΔE vs m_{ES} for the signal MC. The signal box is represented by the solid lines.

In addition to the signal box, we have defined a slightly larger blinding box. The data within the blinding box was kept hidden until the analysis was completed in order to remove any possible experimenter's bias. Finally, we define several sideband regions that will be denoted the fit sideband and the ΔE sidebands. The boundaries of these regions in the $(\Delta E, m_{\text{ES}})$ plane are listed in table 1.

Table 1: The boundaries of the signal box and various sidebands defined for this analysis.

region	ΔE range (GeV)	m_{ES} range (GeV/ c^2)
signal box(SB)	[-0.75, 0.50]	> 5.27
blinding box	[-1.30, 0.70]	> 5.24
fit sideband	[-0.75, 0.50]	[5.10, 5.24]
ΔE sideband (bottom)	[-3.00, -1.30]	> 5.10
ΔE sideband (top)	[0.70, 1.50]	> 5.10

We estimate the background in the signal box assuming that the m_{ES} distribution is described by the Argus function [8]. This assumption is consistent with the observed distributions in the MC and data ΔE sidebands. Due to the correlation between ΔE and m_{ES} introduced by the inclusive reconstruction of the companion B , it is not possible to determine the Argus shape from the ΔE sidebands. Therefore, the Argus parameter is determined from an unbinned maximum likelihood fit using the data in the region defined by $-0.75 < \Delta E < 0.5$ GeV and $5.10 < m_{\text{ES}} < 5.24$ GeV/ c^2 . The Argus shape (A) is extrapolated through the signal box and constrained to be 0 at the endpoint which is fixed at 5.29 GeV/ c^2 . Figure 5 shows the results of the fit. The expected background is given by,

$$N_{\text{bkg}} = N_{\text{fit}} \times \frac{\int_{5.27}^{5.29} A(m_{\text{ES}}) dm_{\text{ES}}}{\int_{5.10}^{5.24} A(m_{\text{ES}}) dm_{\text{ES}}} \equiv N_{\text{fit}} \times R_{\text{Argus}} \quad (6)$$

where N_{fit} is the number of events contributing to the fit. The ratio R_{Argus} is the area of the background probability density function in the signal box divided by the area within the fit region. The result is $N_{\text{bkg}} = 5.0^{+1.8}_{-1.4}$ events. The uncertainty is determined by varying the Argus parameter by the $\pm 1\sigma$ uncertainty from the fit. This technique may underestimate the background since any peaking component within the blinding box would not be accounted for. Therefore, any upper limit obtained on the branching fraction should be conservative. When this procedure is applied to the MC, the resulting background estimate is 5.2 ± 0.5 events, in agreement with the true value of 5.7 ± 0.5 events. The MC indicates the background in the signal box after all cuts are applied is composed of about 58% $q\bar{q}$ (where $q = u, d, \text{ or } s$), 22% $c\bar{c}$ and 20% $B\bar{B}$ events.

4 SYSTEMATIC STUDIES

To set an upper limit on the $B^+ \rightarrow \mu^+ \nu_\mu$ branching fraction we must evaluate systematic uncertainties in the luminosity (number of B^\pm in the sample), the background estimate, and the signal efficiency. The number of B^\pm mesons in the on-peak data sample is estimated to be 88.4 million with an uncertainty of 1.1%. The uncertainty in the background estimate is determined by varying the Argus shape within the $\pm 1\sigma$ uncertainty from the fit.

The uncertainty in the signal efficiency includes the muon candidate selection (particle identification and tracking efficiency) as well as the reconstruction efficiency of the companion B . The muon identification efficiency has been studied using muon control samples taken from $e^+e^- \rightarrow e^+e^- \mu^+\mu^-$ events in the data. For muons in the momentum and polar angle region of our signal candidates, we estimate the uncertainty in the identification efficiency from the control sample to be 4.2%. The tracking efficiency for the muon candidate was evaluated from the fraction of tracks reconstructed in the SVT that are also found in the DCH. We find that the tracking efficiency is overestimated in the MC by 0.8%. Therefore, we reduce the MC signal efficiency by this amount and assume a systematic error of 2%.

The companion B reconstruction has been studied using a control sample of $B^+ \rightarrow D^{(*)0} \pi^+$ events. This is also a two-body decay so it is topologically very similar to our signal. Once reconstructed, the pion can be treated as if it were the signal muon and the $D^{(*)0}$ decay products can be ignored to simulate the neutrino. Then the companion B is reconstructed in the control sample as it would be for signal. We then compare the efficiencies for each of our companion B selection cuts in the $B^+ \rightarrow D^{(*)0} \pi^+$ data and MC to quantify any data/MC discrepancies that may affect the signal efficiency. We find that the efficiency after all selection cuts is lower in the data by a factor of 0.94 ± 0.04 where the uncertainty is due to the statistics of the data and MC

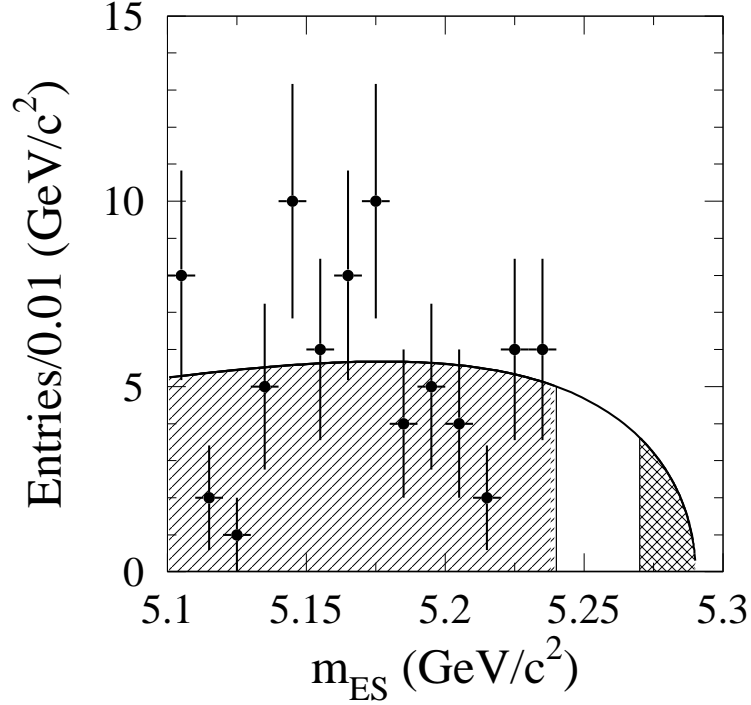


Figure 5: Results of the Argus fit for the background estimate. The fit is performed only on the region $5.10 < m_{\text{ES}} < 5.24 \text{ GeV}/c^2$ (diagonally shaded area) and extrapolated into the signal region represented by the crosshatched area.

control samples. The signal efficiency obtained from the MC is therefore corrected by this factor. A summary of the systematic uncertainties in the signal efficiency is given in table 2. After applying the necessary corrections to the MC, we estimate the signal efficiency to be $2.09 \pm 0.06 \text{ (stat)} \pm 0.13 \text{ (syst)} \%$.

Table 2: Contributions to the systematic uncertainty on the signal efficiency.

source	correction	uncertainty
tracking efficiency	0.992	2.0%
muon identification	-	4.2%
companion B reconstruction	0.94	4.3%
total	0.932	6.3%

5 PHYSICS RESULTS

In the on-resonance data we find 11 events in the signal box where $5.0^{+1.8}_{-1.4}$ background events are expected. The probability of a background fluctuation yielding the observed number of events or

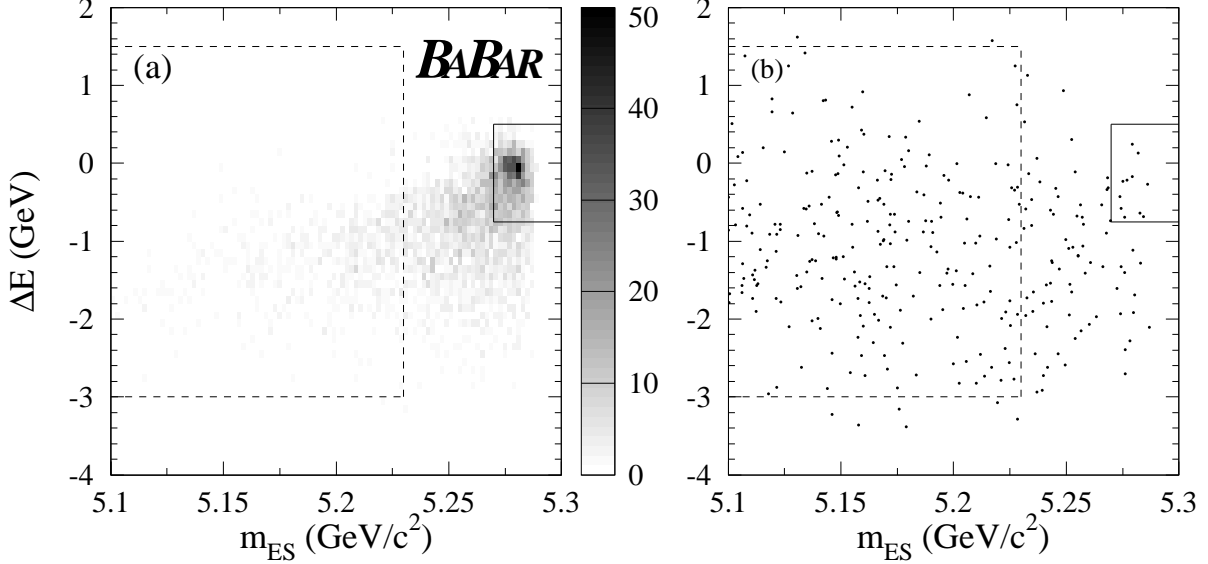


Figure 6: The distributions of ΔE vs m_{ES} in the $B^+ \rightarrow \mu^+ \nu_\mu$ signal MC (a) and the on-resonance data (b). The signal box is represented by the solid line while the grand sideband is represented by the dashed line.

more is about 4%. The distribution of the data in the $(\Delta E, m_{ES})$ plane is shown in figure 6(b). Figure 7 shows the p^* distribution of the on-resonance data after all other selection cuts have been applied. The region between the two arrows ($2.58 < p^* < 2.78$ GeV/c) indicates the selected signal candidates. We set an upper limit on the $B^+ \rightarrow \mu^+ \nu_\mu$ branching fraction using $\mathcal{B}(B^+ \rightarrow \mu^+ \nu_\mu) < n_{UL}/S$ where n_{UL} is the 90% CL upper limit on the number of signal events observed and S is the sensitivity of the experiment which is the product of the signal efficiency and the number of charged B mesons in the sample. To determine the number of charged B mesons we assume equal production of B^0 and B^+ in $\Upsilon(4S)$ decays. Systematic uncertainties are included in the limit following the prescription given in reference [9]. The preliminary result is

$$\mathcal{B}(B^+ \rightarrow \mu^+ \nu_\mu) < 6.6 \times 10^{-6}$$

at the 90% confidence level.

6 ACKNOWLEDGMENTS

We are grateful for the extraordinary contributions of our PEP-II colleagues in achieving the excellent luminosity and machine conditions that have made this work possible. The success of this project also relies critically on the expertise and dedication of the computing organizations that support *BABAR*. The collaborating institutions wish to thank SLAC for its support and the kind hospitality extended to them. This work is supported by the US Department of Energy and National Science Foundation, the Natural Sciences and Engineering Research Council (Canada), Institute of High Energy Physics (China), the Commissariat à l’Energie Atomique and Institut National de Physique Nucléaire et de Physique des Particules (France), the Bundesministerium für

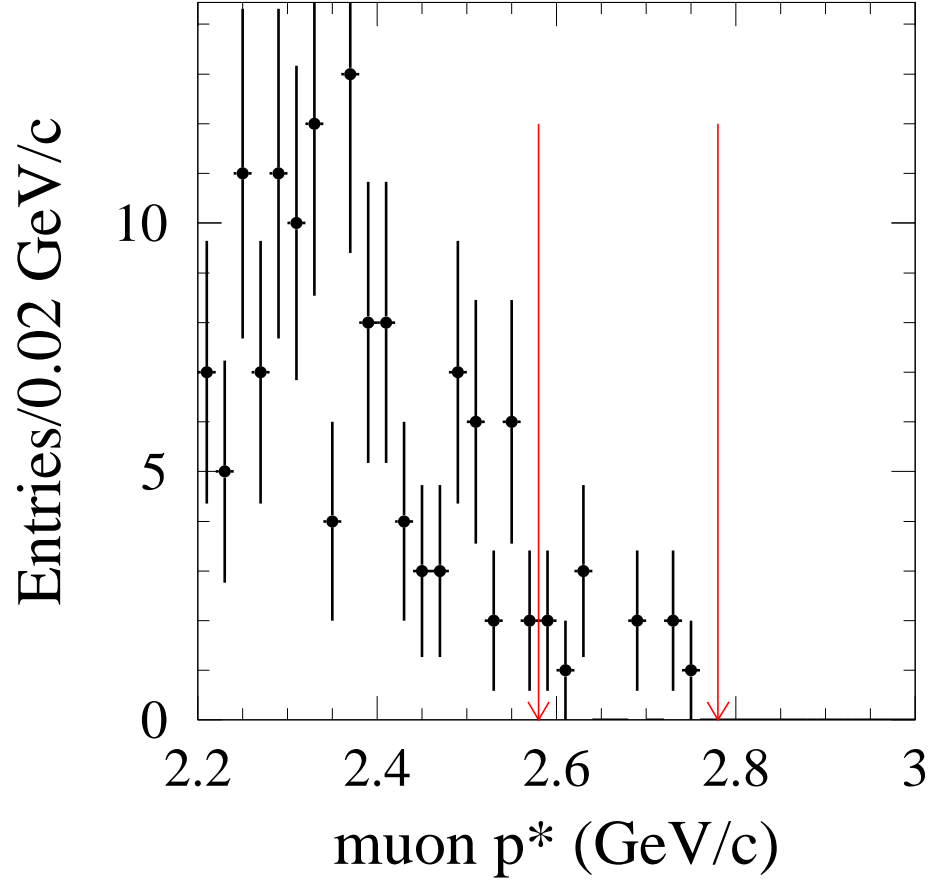


Figure 7: The p^* distribution of the on-resonance data after all other selection cuts have been applied. The region between the two arrows ($2.58 < p^* < 2.78$ GeV/c) indicates the selected signal candidates.

Bildung und Forschung and Deutsche Forschungsgemeinschaft (Germany), the Istituto Nazionale di Fisica Nucleare (Italy), the Foundation for Fundamental Research on Matter (The Netherlands), the Research Council of Norway, the Ministry of Science and Technology of the Russian Federation, and the Particle Physics and Astronomy Research Council (United Kingdom). Individuals have received support from the A. P. Sloan Foundation, the Research Corporation, and the Alexander von Humboldt Foundation.

References

- [1] Particle Data Group, K. Hagiwara *et al.* *Phys. Rev. D* **66**, 010001 (2002)
- [2] W.S. Hou, *Phys.Rev. D Brief Reports* **48**, 2342 (1993)
- [3] G. Valencia and S. Willenbrock, *Phys. Rev. D* **50**, 6843 (1994)
- [4] CLEO Collaboration, M. Artuso *et al.*, *Phys. Rev. Lett.* **75**, 785 (1995)
- [5] The Belle Collaboration, Search for W -Annihilation B Meson Decays, BELLE-CONF-0247
- [6] The BABAR Collaboration, B. Aubert *et al.*, *Nucl. Instrum. Methods A* **479**, 1-116 (2002)
- [7] G.C. Fox and S. Wolfram, *Phys. Rev. Lett.* **41**, 1581 (1978)
- [8] The Argus function is described by,

$$\frac{dN}{dm_{\text{ES}}} \propto m_{\text{ES}} \times \sqrt{1 - \frac{m_{\text{ES}}^2}{E_{\text{beam}}^2}} \times \exp \left[-\zeta \left(1 - \frac{m_{\text{ES}}^2}{E_{\text{beam}}^2} \right) \right], \quad (7)$$

ARGUS Collaboration, H. Albrecht *et al.*, *Phys. Lett. B* **241**, 278 (1990)

- [9] R.D. Cousins and V.L. Highland, *Nucl. Instrum. Methods A* **320**, 331 (1992)